J Fluoresc (2012) 22:685–697
DOI 10.1007/s10895-011-1004-2

ORIGINAL PAPER

Investigation and Development of Quantum Dot-Encoded Microsphere Bioconjugates for DNA Detection by Flow Cytometry

Sarah Thiollet · Séamus Higson · Nicola White · Sarah L. Morgan

Received: 22 June 2011 / Accepted: 18 October 2011 / Published online: 5 November 2011

Abstract The development of screening assays continues to be an active area of research in molecular diagnostics. Fluorescent microspheres conjugated to biomarkers (nucleic acids, proteins, lipids, carbohydrates) and analyzed on flow cytometer instruments offered a new approach for multiplexed detection platform in a suspension format. Quantum dots encoded into synthetic microspheres have the potentials to improve current screening bioassays and specifically suspension array technology. In this paper, commercialized quantum dot-encoded microsphere were evaluated and optimized as fluorescent probes to address some of the limitations of suspension array technologies. A comprehensive study was undertaken to adapt the bioconjugation procedure to the quantum dot-encoded microsphere structural and optical properties. Both the leaching-out of quantum dots and microspheres degradation under bioconjugation experimental conditions were minimized. A rapid, efficient and reproducible conjugation method was developed for the detection of single-stranded DNA with the commercialized quantum dot-encoded microsphere. Approximately ten thousand microspheres were conjugated to short amino-modified DNA sequences in one hour with high efficiency. The bioconjugated microspheres acting as fluorescent probes successfully detected a DNA target in suspension with high specificity. Quantum dot-encoded microsphere commercial products are limited which strongly prevents reproducible and comparative studies between laboratories. The method developed here contributes to the understanding of quantum dot-encoded microsphere reactivity, and to the optimization of adapted experimental procedure. This step is essential in the development of this new fluorescent probe technology for multiplex genotyping assay and molecular diagnostic applications.

Keywords Quantum dot-encoded microsphere · Flow cytometry · Bioconjugation · Suspension array technology

ABBREVIATIONS

D_o	Oligonucleotide density
%	percentage
FSC SSC	forward and side scatter
MES	Morpholino-ethanesulfonic acid
MFI	Median fluorescent intensity
QDs	Quantum dots
QDEM	Quantum dot-encoded microsphere
SEM	Standard error of the mean

Introduction

The use of inorganic fluorophores in bioscience has been hailed as a breakthrough that has had a major impact in the field. Semiconductor nanocrystals (e.g., CdSe, InP, InAs) or quantum dots (QDs) have been highlighted as new optimum fluorescent dyes for biological applications such as immunoassays, bioimaging or molecular diagnostics [1, 2]. QDs were

Electronic supplementary material The online version of this article (doi:10.1007/s10895-011-1004-2) contains supplementary material, which is available to authorized users.

N. White · S. L. Morgan
Translational Medicine Laboratory,
Cranfield Health, Cranfield University,
MK43 0AL Cranfield, UK

S. Higson
Biosensors and Diagnostic Laboratory, Cranfield Health,
Cranfield University,
MK43 0AL Cranfield, UK

S. Thiollet (✉)
Biosensors and Diagnostic Laboratory, Cranfield Health,
Cranfield University,
Check-Points B.V., Wageningen,
The Netherlands
e-mail: sarah.thiollet@check-points.com

described as novel labels for high throughput bioassays because of their remarkable electrical and optical properties due to their material compound, structure and size [3]. QDs have a wide range of emission wavelengths (from 490 nm to 900 nm), with improved signal-to-noise ratio, and narrower bandwidth compared with organic dyes. Mixtures of QDs can be excited with a single source of light (488 nm), which provides a unique spectral code, dependent on the size, composition, and quantity of each of the QD population [4]. Embedded in spherical microspheres structure, such as polystyrene or silica beads that can be solubilized and functionalized, this new type of fluorescent code can be applied to high throughput particle-based bioassay in liquid and solid format. In comparison to previous organic fluorescent bead technologies, quantum dots-encoded microspheres (QDEMs) have the potential to produce a higher number of unique fluorescent codes, because of their higher chemical- and photo- stability, lower limits of detection, and higher level of multiplex abilities [5–7].

Microspheres coated with carboxyl groups have previously been used with suspension array technology for immunoassays and genetic analysis [8]. Suspension array technology has been especially applied to single-stranded DNA identification and quantification using short DNA sequences or oligonucleotides as probes [9, 10]. This method, called allele-specific oligonucleotide hybridization assay, has been previously described with quantum dot-encoded bead and flow cytometry or fiber optic spectrophotometry as detection methods. Briefly, The carbodiimide coupling of DNA probes to carboxylated polystyrene microspheres was followed by the encoding of the microspheres with cadmium selenide (CdSe) QDs in a large production scale (e.g., 50 mg or 20–30 million particles) [6, 11, 12]. These methods were proof of principles, time consuming and costly. Moreover, limitations arose from the biochemistry equipments and processes involved in the developmental strategy needed for the synthesis of the quantum dot microspheres. Despite the advantageous properties demonstrated by QDs and QDEMs as molecular probes and the active research ongoing in this field, extensive commercialized products and validated clinical applications of these materials are not yet available [13, 14]. The main limitations for the development of QD technology to biological applications are related to their synthesis strategies. Until now various methods have been published but none was clearly identified to solve QD technology pitfalls such as spectral broadening, QDs leakage out of the microbeads, energy transfer, quenching effect, or QDs aggregation [15].

To address some of these issues, a new bioconjugation methodology adapted to Crystalplex TriLite™ alloyed nanocrystals-encoded microsphere was developed using flow cytometry detection, in a minute suspension array format. The colors of this new class of "composition-tunable" alloyed nanocrystals are determined by the relative concentration of the elements composing the core of the QDs [14]. Flow cytometer instruments typically have the advantage of low running costs, analyte flexibility, and adaptability to high throughput analysis [8]. The effects of the concentration and the structure of the oligonucleotides attached to the bead were studied to optimize bioconjugation efficiency. Simultaneously, the reactivity and the stability of QDEMs under bioconjugation treatments were analyzed. Then, the QDEM bioconjugates were used for single-stranded DNA detection (Fig. 1). The benefits and adaptability of QDEM bioconjugates for biomedical application are discussed.

Results and Discussion

QDEMs Bioconjugation Study and Optimization

QDs-doped particles could offer a solution to suspension array technology that requires multiplexed fluorescent bioconjugates. A crucial step in suspension array technology development is the optimization of microsphere bioconjugation. Spiro et al. [9] were the first to evaluate conjugation efficiency. Since then, a limited number of studies have investigated bioconjugation efficiency by attaching amino-modified fluorescent oligonucleotide to carboxylated microspheres and using flow cytometry calibration kit [16, 17]. The titration of the probe input is essential to determine the optimal conditions for carbodiimide coupling to a specific type of microsphere and to evaluate the conjugation assay.

A method using Cy3 fluorescent oligonucleotides was developed to assess the coupling efficiency of short DNA probes to carboxylated QDEMs (Crystalplex) (Fig. 1a). The QuantiBRITE Phycoerythrin kit (Becton Dickinson) was chosen for the calibration with the flow cytometer Coulter Epics XL-MCL (Beckman Coulter) because it presented the same detection properties as the Cy3 fluorophore [17]. The organic dyes Cy3 and Cy5 were detected in fluorescent detectors channels FL3 and FL4, respectively, in order to avoid emission overlap with the 525 nm-encoded beads signal detected in FL1. Fluorescence resonance energy transfer, highly dependent on the distance separating the donor of energy to its acceptor, was described between 525 nm QDs (donor) and the Cy3 fluorophores (acceptor) covalently attached through a well-characterized construct [18]. Although the spectral overlap between 525 nm-encoded beads and Cy3 probes was probably ideal and the high level of functionalization could potentially facilitate the interactions described by Clapp et al. [18], Fluorescence resonance energy transfer was considered to

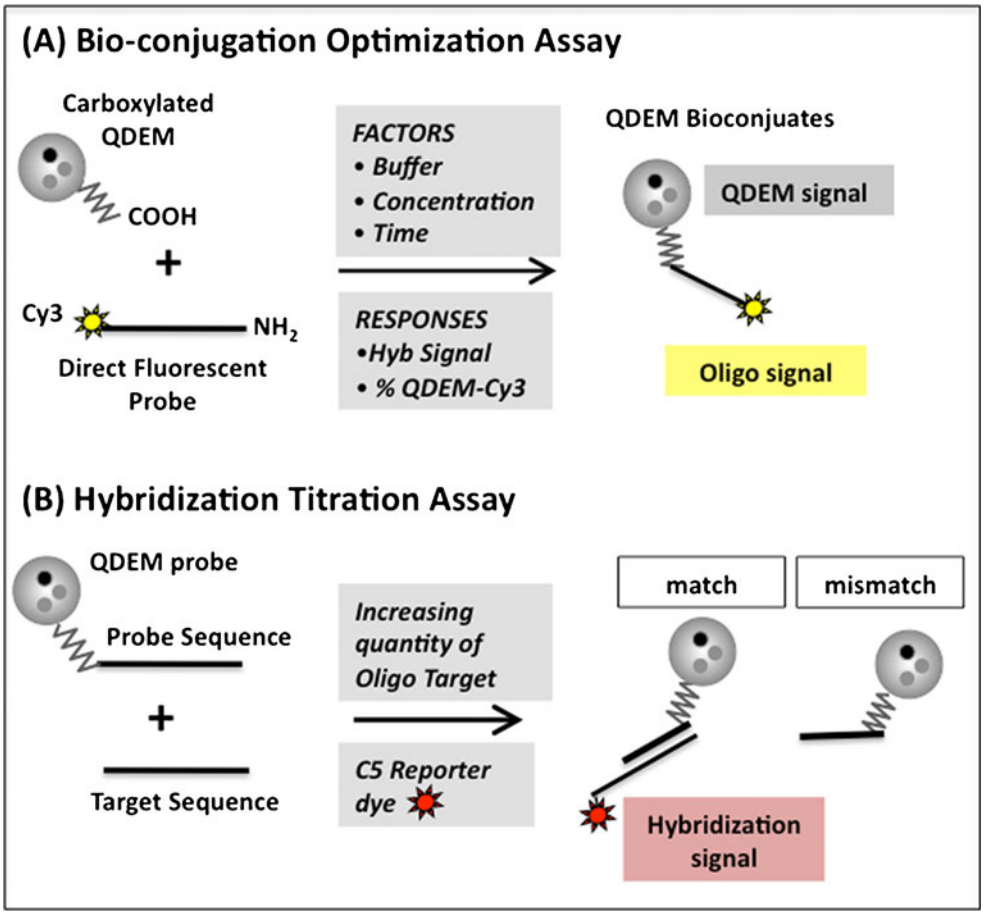

Fig. 1 Experimental strategy, **a** Coupling of oligonucleotides amino group (NH2) with quantum dots encoded microspheres (QDEMs) carboxylated groups (COOH), **b** Hybridization of Cy5-oligonucleotide to matching QDEM-probe. QDEM fluorescent code encoded with TriLite™ quantum dots nanocrystals

have a minor impact because of the distance separating the 525 nm QDs distributed in the microsphere from the Cy3 attached through a carbon spacer and a nucleotidic sequence [19]. The oligonucleotide fluorescent signal on the QDEM surface (corrected median of fluorescence intensity, RMFI in a.u.) was used to calculate the oligonucleotide density on the QDEM surface (D_o in oligo/μm^2) for Cy3 probe quantities ranging from 0 to 400 pmol.

Coupling Buffer and Incubation Time

First, the influence of the coupling buffer on the conjugation efficiency was evaluated by comparing two of the most common carbodiimide buffers: 2-(N-Morpholino) ethanesulfonic acid or MES buffer and imidazole (Fig. 2). The imidazole titration curve presents a coupling saturation point at 200 pmol with a maximum D_o of ~12,588 (±2,477) oligo/μm^2. The MES coupling saturation point requires the same quantity of probes as with imidazole but shows a D_o max (4,796 (±343) oligo/μm^2) almost three times lower. At the time of writing, no quantitative coupling efficiency studies were reported with QDEMs, but a mean signal of ~300,000 to 500,000 oligo/bead was described with 5.5–5.6 μm diameter beads (Bang Laboratories, Fisher, IN, USA) corresponding to a D_o~2,865–4,775 oligo/μm^2 [20]. Further, a specific study in MES buffer was carried out by Wittebolle et al. [16] using 100,000 polybead of 3 μm diameter (Polysciences, Warrington, PA, USA) with a D_o max~1,345 (±112) oligo/μm^2. Luminex technical application group, specialized in suspension array technology and organic fluorescent bead technology, functionally assessed coupling efficiency by the hybridization of biotinylated oligonucleotide labeled with streptavidin-Phycoerythrin complementary to the probe attached on the bead surface encoded with organic dyes [21]. This method for probe titration is therefore based on an indirect reaction, which potentially introduce a bias in the oligonucleotide-microsphere coupling recommendation [9]. The method presented in Fig. 1, measures the direct fluorescent signal of probes conjugating to the bead surface, which should provide more accurate conjugation efficiency results.

The maximum conjugation efficiency obtained with QDEMs was 2.6 to 4.4 times higher in imidazole buffer, and 10 times superior with MES buffer in comparison to previous work [9, 16]. Heterogeneity in the carboxylation coverage of the beads could partially explain these differences. The results of the acid/base titration indicated a

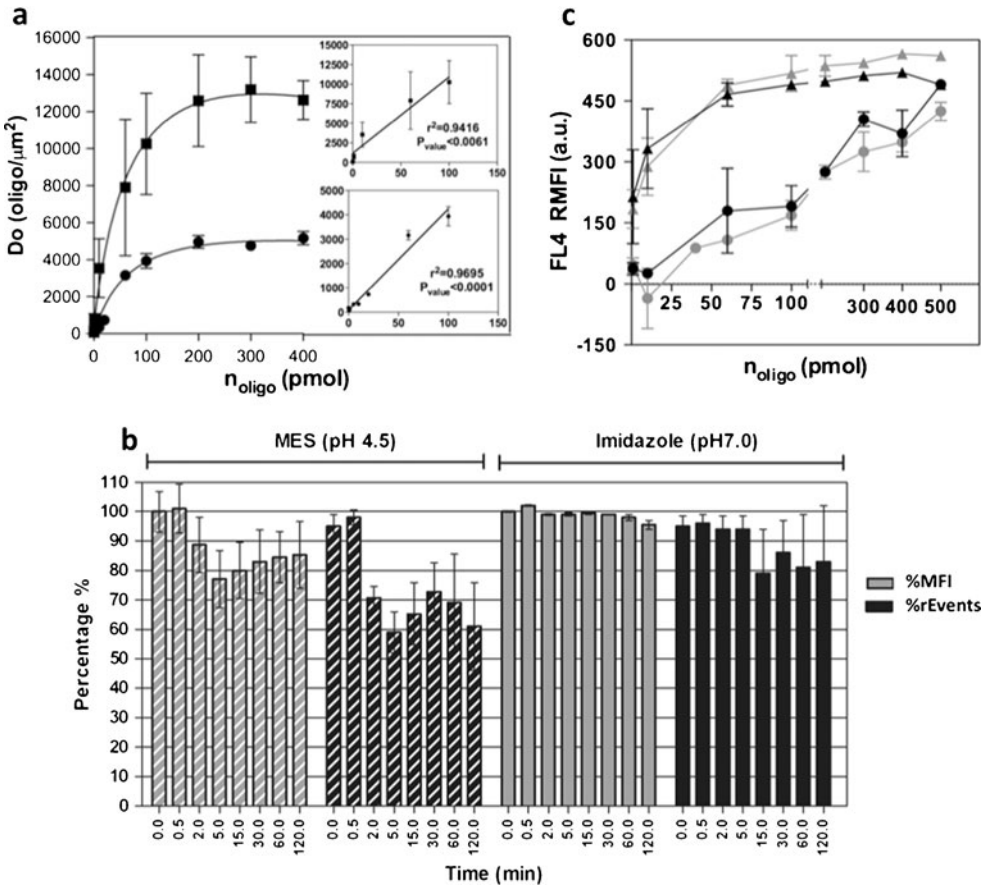

Fig. 2 Impact of the conjugation buffer and probe carbon spacer on QDEM bioconjugation, **a** Titration *curve* of QDEM conjugation to Cy3-oligonucleotide in (■) imidazole and in (●) MES buffer. *Curves* showing the Do (in oligo/μm^2) function of the oligonucleotide quantity (n_{oligo} in pmol) were independently obtained using a non linear regression fit model. The insets show the linear regression for probe quantity before saturation. Data are presented as the D_o±standard error of the mean (±SEM) of 3 replicates. The x unites of Cy3 brightness at saturation was equivalent to y MEFs of phycoerythrin under the conditions used; **b** The relative MFI (%FL) and the relative percentage of events (%rEvents) of 525 nm-encoded beads incubated in MES and imidazole buffer over time (in min). Data are presented as the mean (±standard error) of 3 replicates; **c** The corrected mean of fluorescence intensity (RMFI, in arbitrary unit) versus oligonucleotide probes (pmol) with 6 or 18 carbon spacer such as (▲6C; ▲18C) in Imidazole and (●6C; ●18C) in MES. Cy5 reporter dye was detected in FL4. Data are presented as the RMFI (±standard error) of 3 replicates

relative high carboxyl groups density of ~26.3 microequivalent per gram (μeq/g) compare to other carboxylated dyed microspheres [20]. Steric hindrance and/or the maximum limit of microsphere carboxylation depending on manufacturers could also explain a physical saturation observed with high quantity of fluorescent probe (200 to 300 pmol). Further, a high concentration of Cy3 molecules spatially close on the QDEMs surface could lead to self-quenching or fluorescence saturation between identical fluorophore species [22].

The graph in Fig. 2b shows that after 2 min of incubation with MES buffer the relative percentage of events of QDEM population (%rEvents) started to decrease, reaching a minimum of ~77% (±10) after 5 min. Similarly the relative MFI expressed as the percentage of median fluorescent intensity (%MFI) decreased after 2 min and stays low with longer incubation times, ranging from ~50% (±16) to 28% (±10). Incubation in imidazole buffer showed less impact on the structural and fluorescent stability of the QDEMs: after 2 h the %MFI decreased of only ~5% (±2), whereas the %rEvents decreased of ~15% (±21) after 15 min. QDEMs were more stable in imidazole than in MES conjugation buffer (Fig. 2b). The benefit of increasing the incubation time from 1 h to 1 h30 was also investigated showing no significant improvement in the conjugation efficiency (data not shown). The results presented in Fig. 2 demonstrate the superiority of the imidazole buffer over MES for QDEM stability and conjugation efficiency.

Carbon Spacer Benefit

The carbon spacer that separates the oligonucleotides from the microsphere is described as a flexible structure, resistant to bending or shortening, and is reported to minimize steric and electrostatic interferences between the two entities [23].

Previous work demonstrated that a carbon spacer arm (>6 C) significantly enhanced the carbodiimide coupling reaction [19]. Cy5 probes with 6 C and 18 C spacer arm were conjugated in imidazole and MES buffer to 525 nm-encoded beads in a range of 0 to 500 pmol, to investigate the effect of carbon spacer on coupling (Fig. 2b). The qualitative analysis of the Cy5 probes signal (RMFI detected in FL4) showed no significant increase of the fluorescence for the probes with a 18 carbon spacer after 1 h. The experiment also confirmed that the imidazole buffer was the most efficient buffer: the RMFI was ~500 a.u. with imidazole against ~200 a.u. with MES buffer for 100 pmol of Cy5 probe.

Conjugation Specificity and Optimization

A linear quantitative relationship was found between direct labeled probe quantity and the D_o (r^2=0.941 for imidazole and r^2=0.969 for MES) in the dynamic range of 0 to 400 pmol (insets Fig. 2). From these results, the oligonucleotide quantity needed to obtain approx the equivalent of a third of the D_o saturation value, i.e. 60–70 pmol, was chosen to provide an optimum probe coverage while avoiding fluorescent and steric inhibition during the hybridization process due to probe saturation [23]. To evaluate the specificity of the imidazole conjugation method, the activators were replaced with clean water (H_2O). No significant background noise was detected with confocal microscopy in the optimum oligonucleotide range, i.e. 60–70 pmol (Fig. 3). The FL2 background signal of the 525 nm encoded beads stock solution detected with flow cytometry was very low and equivalent to the fluorescence detected with 0 pmol of Cy3 probe. A maximum of 11% non-specific binding was detected at saturation (Additional file 1). Non-specific binding with high concentrations of fluorescent probe could illustrate the natural tendency of cyanine fluorophores to react with polymer surfaces without activators [16], and/or the interaction of QDEM carboxyl groups with the amino groups carried by the oligonucleotides [24]. Non-specific binding was limited by storing the QDEMs in a buffer containing 1% bovine serum albumin (BSA). Native BSA has shown useful blocking agent properties in microsphere covalent binding assays by covering hydrophobic surface and avoiding non-specific interaction [24]. The QDEM conjugation assay was highly specific and sensitive with the optimal conditions of 65 pmol of a 6 C amino-modified conjugation probe and 1 h incubation in imidazole buffer.

Evaluation of the QDEM Bioconjugation Procedure

Conjugation was undertaken for 11 replicates with the optimum conditions defined previously. Samples were run on the flow cytometer and a gate was defined with the non-encoded beads and the 525 nm-encoded beads control population before treatment. The number of events and the median fluorescent intensity (MFI) data were collected on the control and bioconjugates gated population. MFI data reported in the channel detector FL3 and FL4 were excluded from the statistical analysis because the MFI was close to 0 for both control and bioconjugates.

Comparing QDEM Fluorescent Code of Control Population to Bioconjugates

The effect of the bioconjugation procedure on the QDEMs was systematically evaluated by comparing a control population against treated QDEMs using a t-test. A

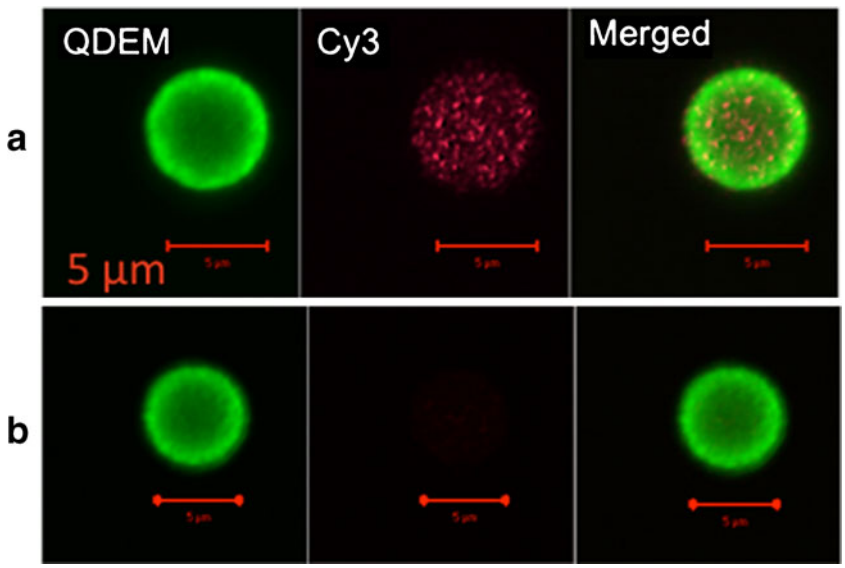

Fig. 3 Confocal images of **a** the positive and **b** the negative control of 525 nm-encoded beads conjugated with 65pmol of Cy3-probe (5 μm *red scale bars*)

marked shift of the fluorescence intensity in both FL1 and FL2 was observed after attaching oligonucleotide probes to non-encoded beads (Fig. 4a). The specificity of the code identification and the sensitivity of the target detection in suspension assays are typically limited by the amount of background noise detected on the bead population at a specific wavelength. Potential non-specific binding on the microspheres surface was found to be blocked by the 1% BSA present in the QDEM storage buffer (Fig. 3). The significant increase of MFI in FL1 and FL2 for non-encoded beads bioconjugates (Fig. 4a) was therefore mainly composed of autofluorescence: the fluorescence associated to the microsphere substrate and the attached DNA target [25, 26]. The difference in the means increased of ~144 (±30) a.u. for FL1 with (p=0.0112) and of ~193 (±11) a.u. for FL2 with (p<0.0001).

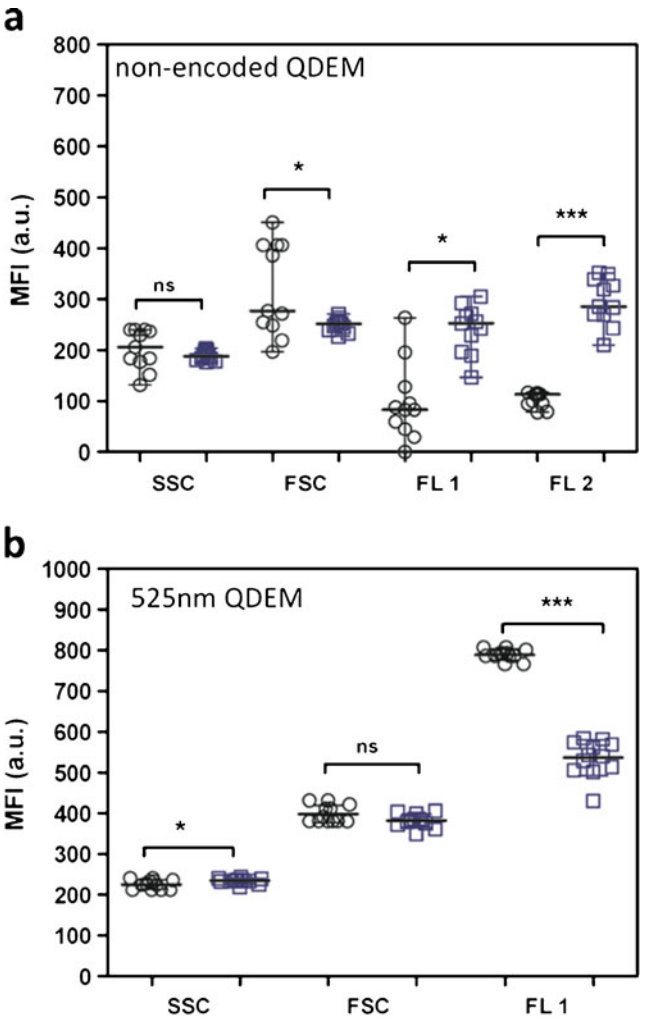

Fig. 4 MFI data scatter plots and *t*-test comparison between (□) QDEM bioconjugates and (○) control population for **a** non-encoded and **b** 525 nm-encoded beads replicates. Data are presented as the median (±standard deviation); horizontal lines mark the median; asterisks represent the significance level related to the p-value. *ns* not significant (p>0.05), * significant at p<0.05, *** significant at p< 0.001 (see Additional file 2)

In contrast, the fluorescence code of 525 nm-encoded beads bioconjugates detected in FL1 decreased significantly (p<0.0005) in comparison with the control, with a mean difference equal to a diminution of ~253 (±14) a.u. (see Additional file 2) (Fig. 4b). Modifications of the forward and side scatter (FSC and SSC) between control and bioconjugates were also observed: the FSC emission for non-encoded beads was significantly lower (~−71 (±28) a.u.) with bioconjugates (p=0.0271) (Fig. 4a), whereas increase of SSC emission was observed with 525 nm-encoded beads bioconjugates (increase of ~9 (±3) a.u) and (p<0.05) (Fig. 4b).

The statistical results presented in Fig. 4 were confirmed with confocal images of 525 nm-encoded beads bioconjugates (Fig. 5a). The typical heterogeneous QDEM-bioconjugate population was composed of: normal QDEM (n°1) with uniform distribution of the 525 nm emission (in green) and Cy3 signal (in red), QDEMs with different green fluorescence intensity (n°1 and n°2), beads that have lost the green fluorescence but emit the red signal of the Cy3-probe (n°3), and beads displaying a broken shell structure (n°4).

Chemicals and treatments applied to the 525 nm-encoded beads population, i.e., buffer, washing steps, vortex, and sonication, can provoke the washing out of the QDs out of the beads, which could be the main factors contributing to the decreased of fluorescence observed here [22, 27, 28]. The main effects produced by ultrasound sonication are: heat, cavitation, agitation, acoustic streaming, interface instabilities and friction, diffusion and mechanical rupture. All these effects impact on the polystyrene/methacrylate microsphere stability [29, 30]. The impacts of ultrasound sonication or sonochemical changes in the polystyrene matrix of the beads associated to sonomechanical forces could modify the distribution of the QDs in the microsphere and cleave polymer chains in solution [31]. The commercial QDEM tested here were produced with the most common QD-doped particle synthesis strategy. Briefly, QDs are captured physically by diffusion inside a polymer matrix, the polystyrene microsphere, with solvent swelling of the microbeads. Then, a chemical sealing layer is added to the beads surface [5]. Sonication and treatment with polar or non-polar solvents could therefore result in a loss of QDs from the microsphere due to swelling, the absence of chemical bound between the QDs and the polymer matrix of the bead, and changes in the bead macrostructure. Alternative synthesis strategies using silica materials are more stable but not adapted to suspension array technology because of the poor dispersion of silica beads in solution [32].

Figure 5a also illustrates the differences of intensity of the Cy3-probe signal between beads. QDEMs with orange

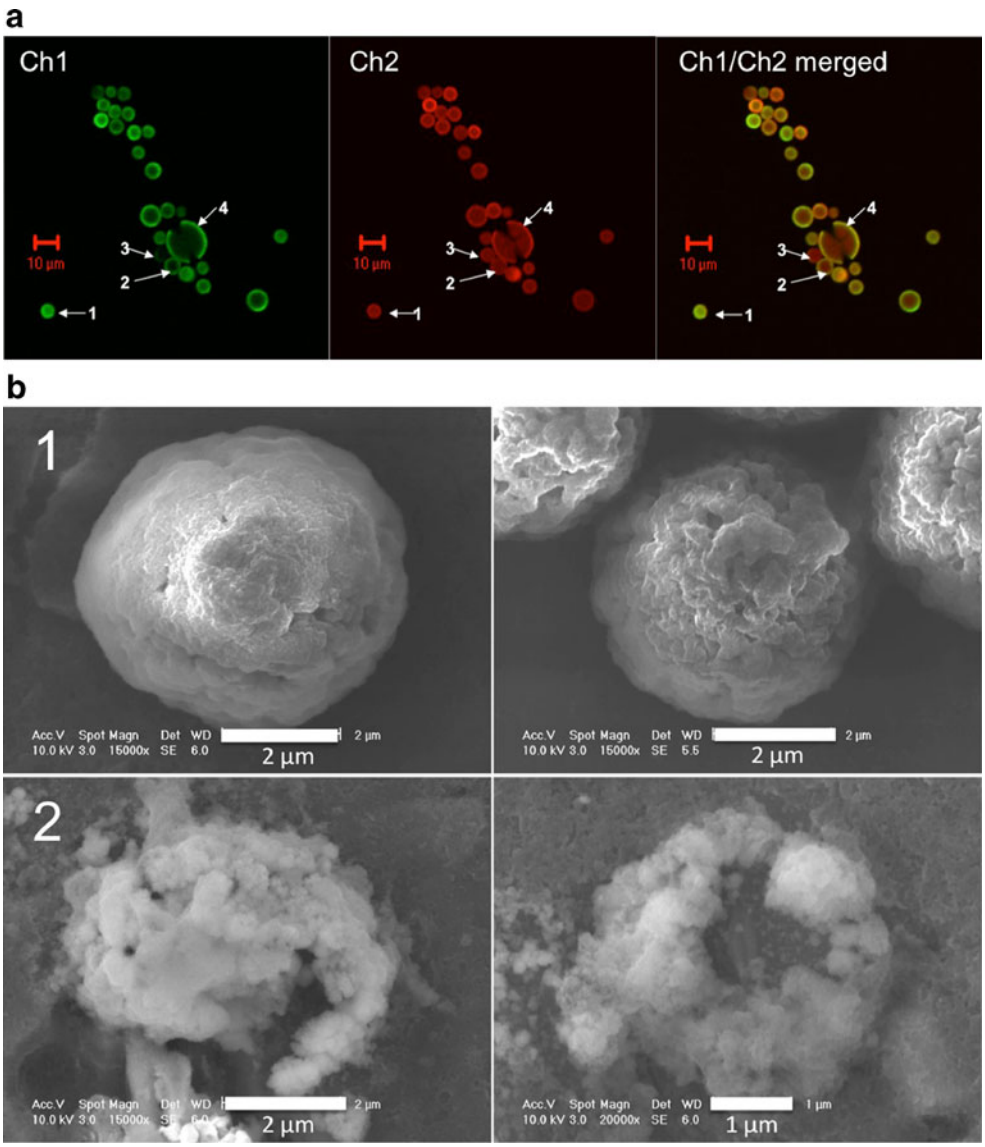

Fig. 5 Microscopy images of QDEMs and QDEM bioconjugates, **a** True color imagines obtained with confocal microscopy of 525 nm-encoded beads bioconjugates and **b** Scanning electron micrographs [1] before and [2] after treatment. Scale bars were redrawn for clear observation. Ch1: channel 1 (*green spectra*) detects 525 nm-encoded beads, Ch2: channel 2 (*red spectra*) detects the Cy3-probe fluorescent emission. Different QDEM bioconjugate profiles are indicated with *white arrows* and *numbering*

and greener photoluminescent profile are shown in Ch1/Ch2 merged image, which could suggest a lack of uniformity in the performance of the fluorescent probe conjugation to the QDEM.

The impact of the QDEM fluorescence code modifications due to the bioconjugation procedure, such as autofluorescence, washing-out of the QDs and biochemical structural modification could be a limitation to the performance of the QDEM assay. The changes in non-encoded beads and 525 nm-encoded beads emission signals raises the risk of encroachment of the fluorescent codes when the number of QDEM codes increases, but also when the complexity of the QDEM codes detection intensifies. The potential overlap of fluorescent profiles could reduce the multiplex capabilities of the QDEM fluorescent encoding technology. The impact of encroachment upon bead signals for a subset of QDEM before and after bioconjugation could be modeled and empirically evaluated to optimize code detections adapted to QDEM bioconjugates. The encroachment on the analyte signal is not expected to be significant if effective gating and mean analyte signal algorithms are employed [33]. Consequently, we recommend using the QDEM bioconjugate population as a reference to specifically design flow cytometery protocols and gates for the different colored QDEM populations in order to successfully plot and collect the MFI of multiple QDEM-bioconjugate in large-scale screening assay. Ideally, quantum dot-encoded bead experiment would require fluorescent standards for the characterization and performance validation of the assay depending on the analytical fluorescence instruments used. Such standards would enhance the comparability of fluorescence data, and enable quantitative analysis [34, 35].

Impact of Bioconjugation on the QDEM Structural Stability

The percentage of events (%Events) between QDEM samples treated identically was compared using the row data (Fig. 6a). The %Events significantly decreased in the bioconjugates population in comparison with the control 525 nm-encoded beads (20% (±4)). The number of non-encoded beads also significantly decreased of ~29% (±4) after treatment. The effect of the procedure on non-encoded beads and 525 nm-encoded beads was compared with a *t*-test and no significant difference of %Events was found between non-encoded and 525 nm-encoded beads control, and between non-encoded and 525 nm-encoded beads bioconjugates ($p>0.05$) (Fig. 6a). The observations made on the bead stability were therefore independent of the QDEM fluorescent code.

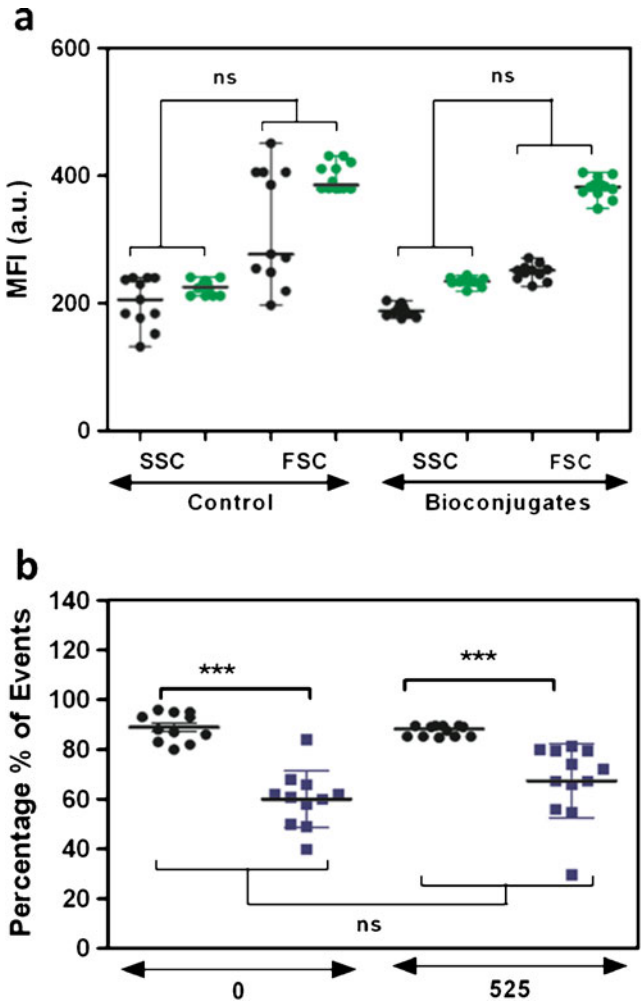

Fig. 6 Scatter plot comparing **a** the %Events of (●) non-encoded beads and (●) 525 nm-encoded beads, and **b** the side and forward scatter MFI of (■) QDEM bioconjugates and (●) control population. Full statistical data available (see Additional file 2). Data are presented as the median (±standard deviation); *horizontal lines mark* the median; *asterisks* represent the significance level related to the p-value. *ns* not significant ($p>0.05$), * significant at $p<0.05$, *** significant at $p<0.001$

Broken microsphere structures were observed in the bioconjugate population and identified as damaged materials with confocal microscopy images and scanning electron microscopy (Fig. 5a, b). QDEM bioconjugate under high resolution scanning electron microscopy present a rough surface (Fig. 5b1). Figure 5b2 reveals a partially spherical microsphere and a broken structure in the bioconjugate samples. The comparison between the micrograph b1 and b2 demonstrates significant modifications of the microsphere shape, size and structural appearance, typically observed in QDEM-bioconjugate population. As previously described, the sonication/vortexing repeated treatment applied during bioconjugation was believed to initially weaken the structure of the polystyrene microsphere. QDEMs would therefore be more sensitive to swelling with the diffusion of water molecules and chemicals component in the weakened structure, leading eventually to the bursting of microspheres (Fig. 6).

Here, we demonstrated that QDEMs are unstable under bioconjugation treatment. The destruction of the bead chemical shell was found to be one of the main mechanisms responsible for the diminution of the percentage of events after bioconjugation. The diminution of the number of QDEM-probes implies a loss of quantitative and qualitative information, and it is also cost inefficient. The effect of the overall bioconjugation procedure was evaluated to assess the method efficiency. The mean of the relative percentage of fluorescence and events was calculated with all QDEMs replicates before and after bioconjugation (Table 1). These results establish the importance of the optimization work presented in this study. It also demonstrates that the choice of buffer and handling procedure have been improved because ~75% of the initial QDEM population were recovered at the end of the procedure.

Evaluation of the Bioconjugation Procedure Reproducibility

FSC and SSC corrected median fluorescent intensity (RMFI, in a.u.) data were compared to evaluate statistical differences among populations (Fig. 6b). Non-encoded beads FSC significantly decrease and 525 nm-encoded beads SSC significantly increase with low significance level ($p=0.0271$ and 0.0291). The initial structural and optical differences between non-encoded and 525 nm-encoded beads, due to the encoding process, could have an impact on their specific response to light scattering, leading to a different pattern of FSC and SSC variations upon treatments.

FSC is mainly proportional to the size and shape of the detected particles. The larger the QDEM, the more light is

Table 1 Statistical differences between 525QDEM controls and bioconjugates

525QDEM	FL		% Events	
	Control	Bioconjugate	Control	Bioconjugate
Lower 95% CI[a] of mean	780.7	508.1	86.1	57.9
Upper 95% CI of mean	797.6	564.2	88.75	76.8
Relative % CI of mean	~65–71		~67–87	

[a]*CI* confidence interval; CI data available in Additional file 2

scattered, hence the higher the MFI [36]. The increase in FSC was expected with bioconjugates since size and external shape could be modified by the attachment of the oligonucleotides on the bead surface and by the effect of the procedure on the bead structure. The flow cytometer instrument could have missed the FSC variations of the 525 nm-encoded bead populations if these variations were in a constrained range of values inferior to the standard limit of detection. These limitations could explained the statistical results showing a p=0.069 with a very low level of non-significance, just above the 5% limit. The flow cytometry limit of detection also explained the general low level of significance observed with FSC and SSC analysis when comparing 11 replicates within a single population (Fig. 6b).

Therefore, non-encoded and 525 nm-encoded beads were grouped as a single population to evaluate the general impact of the bioconjugation procedure on QDEMs and no significant differences were observed between control and bioconjugates for both FSC and SSC. Likewise, no significant variation of the %Events was observed (Fig. 6a). However, individual analysis of each bead population showed that both QDEMs population were affected by the treatment, and that bead recovery was lowered by approx 20% (Additional file 2).

First, the absence of differences between the observed variations before and after treatment in 0 and 525 nm-encoded bead populations illustrated the reproducibility of the bioconjugation procedure for separated batch experiments. Second, the stability of FSC and SSC signals, as well as the %Events variations were found to be independent of the QDEM fluorescent code. These observations can be explained by the identical post-encoding synthesis procedure applied to blank and color bead. The same protective layer is applied to both encoded and non-encoded microsphere as a sealing procedure (personal communication with J. Crawford, Crystalplex, USA). These results also stressed out the importance of the chemical composition of the encoded microsphere-sealing layer to avoid QDs leakage under environmental stress conditions.

Hybridization Assay

QDEM bioconjugate probes were tested for the identification of a 196 bp single-stranded DNA target, amplified by polymerase chain reaction (Fig. 1b). The impact of the DNA target quantity on the hybridization signal was evaluated (Fig. 7). The hybridization signal was detected with~30 fmol, which is superior to the average limit of 37 fmol described by Horejsh et al. [37] with a molecular beacon bead-based assay for DNA detection on flow cytometer, and largely superior to the 0.5 ng of PCR products necessary to obtain the correct genotype of one single nucleotide polymorphism with the single base chain extension microsphere-based assay reported by Chen et al. [38]. The identification of the Y- single nucleotide polymorphism genotypes of the DNA templates was undertaken by signal-to-noise analyses (Fig. 7). The relative hybridization signal was significantly higher with the matching probe (>50 a.u.) than with the non-matching probe. The average signal-to noise ratio for non-specific hybridization signal was half of the average signal-to-noise ratio found in the literature for comparable single nucleotide polymorphism assay [39, 40].

Contribution to the noise signal is dependent on the oligonucleotide sequence of the probes and the target, and on the type of mismatches because some are more destabilizing than others [41]. The flanking regions of the targeted sequence can also contribute to increased non-specific hybridization in DNA genotyping assays, which

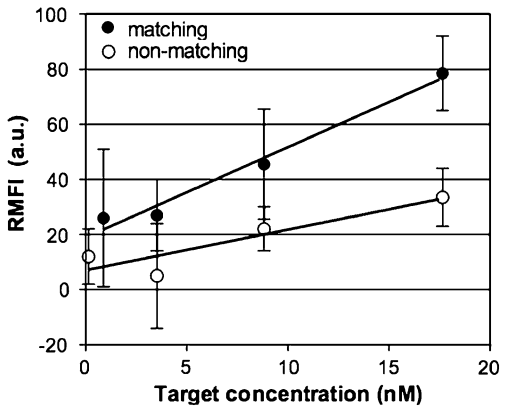

Fig. 7 Linear regression plot of the corrected mean of fluorescence (RMFI, in a.u.) function of oligonucleotide concentration (in nmol/L or nM). Hybridization titration of QDEM matching and non-matching probe to the single nucleotide polymorphism target. Fluorescent hybridization signal detected in FL4. Data are presented as the RMFI (±SEM) of 3 replicates

potentially contribute to background noise and reduce sensitivity [39]

The experiments conducted in this study represented an initial demonstration of the potential of QDEMs applied to hybridization assay in suspension. To improve hybridization sensitivity, other factors has to be considered such as: the type of detection method, beads diameters, carboxylation coverage, probes and target length, but also the method chosen to evaluate assay accuracy, reproducibility and sensitivity. Following the development of stable QDEM-bioconjugates presented here, an allelic suspension oligonucleotide hybridization assay adapted to commercialized QDEMs was developed. A novel optimization approach was used that simultaneously maximize hybridization efficiency and the stability of the materials [42].

Conclusion

In this study, we investigated the adaptability of the first commercial QDEMs to bioassay application, focusing on the evaluation of the technology for suspension array and DNA detection. We have demonstrated that TriLite™ QDEM can be conjugated to short oligonucleotide probes in 1 h with high efficiency. The empirical evaluation of the fluorescent probe technology was necessary to develop and optimize the bioassay adapted to QDEM structural characteristics. The specificity and stability of the probe's fluorescent code are essential for the ability of the researcher to follow the specific signature of the probes along the experimental process. The impact of the treatments applied to the QDEM during bioconjugation was minimized through the selection of optimal conditions adapted to quantum dot-encoded bead structural and optical sensitivity. The method was reproducible with an average of ~75% of the QDEM fluorescent codes recovered at the end of the bioconjugation assay. Here, we also demonstrated that the optimization of minute quantities of QDEM-bioconjugates allowed the specific detection of DNA biomarker in solution. Since the production of QDEMs is still under development and incurs high cost, this step was essential for the future development of a high throughput method and for the detection of samples poor in DNA content. A limited number of reports mentioned the instability of the QD-doped particles in aqueous environment and no specific study was reported until now. The development of a bioconjugation and hybridization assay adapted to a specific type of commercialized quantum dot-encoded microspheres contributed to further development and comparative studies of QD-doped particles. Future developments of the method include the application of the bead-based assay to multiplex single nucleotide polymorphism assay and computational data analysis to demonstrate the potential of commercialized QDEMs for DNA genotyping and molecular diagnostics.

Experimental

Chemicals and Instrumentation

Conjugation probes were designed with: (i) a 5′ amino group for coupling to carboxylated microspheres, (ii) a 5′ carbon spacer (6 C or 18 C carbon), (iii) a universal sequence in addition to a 18-mer polyadenine (poly(A)) sequence, and with or without (iv) a 3′ cyanine fluorophore (Cy3 or Cy5). Two non-fluorescent allelic probes were designed with Primer3 [43] for the identification of a single nucleotide polymorphism on the Y chromosome (database SNPs accession number rs2032623, -/T allele frequencies of 0.926/0.074 (dbSNP, www.ncbi.nlm.nih.gov/projects/SNP/)). The component (iii) was replaced by the specific allelic sequence for each probe. Primers were designed with Primer3 to amplify a 196 base pair target sequence. The reverse primer was biotinylated on the 5′ end (PCR specifics, oligonucleotide sequences and reference are available in Additional files 3). A streptavidin linked to fluorophore cyanine 5 was used as a reporter dye to identify the hybridized complex (Fig. 1b) (Sigma Chemical, Co, Poole, Dorset, UK). Oligonucleotides were purchased from Thermo Electron (Bremen, Germany). Experiments using organic dyes were performed in the dark.

Carboxylated polystyrene microspheres (QDEM) of 5 μm (±10%) diameters encoded with TriLite™ alloyed nanocrystals (CdS_xSe_{1-x}/ZnS core/shell), and non-encoded microspheres (blank) were purchased from Crystaplex (Pittsburgh, PA, USA). QDEM solutions were quantified as previously described using a Neubauer haemocytometer (Reichert, Bright-line®, New-York, NY, USA) [8].

Characterization of QDEMs

The carboxylation coverage of the QDEM surface was determined by acid–base titration. 6 μL of QDEM stock solution (1.46×10^7 bead/mg) was mixed at room temperature with 5 mL of 0.8 mM sodium hydroxide (Fisher, Loughborough, UK) and titrated with 1 mM of chloride acid (Fisher) until the acid–base equivalent point was determined potentiometrically; the microequivalents of carboxyl groups per gram of particles were then calculated.

QDEM samples were analyzed in 400 μL of 0.1 M tris-ethylenediamine tetra acetic acid (TE) pH 8.0 (Fisher) on a Coulter Epics XL-MCL flow cytometer (Beckman-Coulter, Miami, FL, USA). In this study, the organic dyes Cy3 and Cy5 because they were detected in fluorescent detector channels FL3 and FL4, respectively, in order to avoid

emission overlap with the 525 nm-encoded beads signal detected in FL1.

Scanning electron microscope (Philips XL-30 Environmental scanning electron microscope, Philips Electronics, Netherlands) and scanning confocal microscope (Axioskop2-plus LSM 510, Zeiss, Berlin, Germany) were used to characterize QDEM. Samples for scanning electron microscopy analysis were washed in a 50% methanol solution, resuspended in methanol, and deposited on an aluminum plate. With the confocal microscope, channel 1 (green spectra) detected 525 nm-encoded beads, excited at 488 nm (Argon laser, 2% power intensity) with a 505–530 nm band pass filter, whereas channel 2 (red spectra) detected direct Cy3 probes excited at 543 nm (HeNe Laser, 60% intensity) with a 560–615 nm band pass filter on superfrost color slides 76×26 mm, with coverglass 22×50 mm (Menzel-glaser, Braunschweig, Germany). Blank or non-encoded QDEMs were used to normalize the fluorescence and define the background noise. QDEM solutions were systematically resuspended before analysis and a minimum of 10 beads of each sample were observed for microscopic analysis.

A volume equivalent to 10,000 QDEMs calculated from the stock solution was used to test the coupling buffers. 525 nm-encoded beads were incubated in 25 μl of MES (pH 4.5) and imidazole (pH 7.0) at room temperature for 0 to 2 h, while shaking at 400 to 600 rpm. This time range was chosen to illustrate the average incubation conditions used in the literature for high throughput carbodiimide coupling, which typically required a minimum of 30 min to a maximum of 2 h incubation time [8, 11, 15, 18, 19]. After incubation tests, QDEMs were centrifuged for 1 min at 8,000 rpm and resuspended in TE buffer (10 mM Tris-Cl, 1 mM EDTA, pH 8.0, Sigma) for flow cytometry analysis

Coupling of QDEMs to Oligonucleotides

The method (Fig. 1a) was adapted from Spiro et al. [9]. A volume of 10,000 525 nm-encoded beads emitting at 525 nm (Crystalplex) was conjugated by amino-carboxy coupling to a range of 1 to 400 pmol of direct fluorescent probes in 20 μL of 2[N-Morpholino] ethanesulfonic acid (MES) pH 4.5 buffer (Sigma Chemical, Poole, UK). Centrifugations were performed at 1133× g for 4 min. QDEM solutions were systematically resuspended in solution by 15 s of vortex and 20 s of sonication, repeated three times; 2 μL of fresh carbodiimide activators, i.e.,1-ethyl-3-(3-dimethylaminopropyl)-carbodiimide (EDC, 10 mg/ml in nuclease free water (H_2O), Sigma) and sulfo-*N*-hydroxysuccinimide (sulfo-NHS, 10 mg/ml in H_2O, Sigma), were added to the mix and incubated for 30 min at room temperature shaking at 500 rpm (MS1 shaker, IKA®Works, Wilmington, WC, USA). The previous step was repeated and samples were then washed at room temperature (3 min, 400 rpm) successively in 400 μL of 0.02% Tween-20, 0.5% sodium dodecylsulfate (SDS), and 0.1 M of TE. The previous protocol was repeated with imidazole pH 7.0 coupling buffer (Fisher). After incubation, samples were washed (RT, 4 min, 400 rpm) twice in imidazole and once in 0.1 M TE. Three types of negative control were used. QDEM stock solution and QDEM incubated with H_2O evaluated the fluorescent noise inherent to the flow cytometer and the effect of the procedure on the QDEM emission signal. QDEM incubated with fluorescent probe but without the carbodiimide activators estimated the fluorescent background due to non-specific binding. Negative controls were performed for each batch experiment.

Hybridization Assay

The titration of two single-stranded DNA sequences (the probes) differing by one mismatch to the complementary sequence (the target) was performed to evaluate the hybridization sensitivity and specificity of QDEM probes. Non-encoded and 525 nm-encoded microspheres were conjugated respectively to the matching and non-matching probes. 1 μL of a QDEM population (9×10^3/μL) was resuspended in 15 μL of prewarmed 6× standard saline citrate (20× SSC, pH 7.0, Sigma, 0.5% SDS (pH7.0)) hybridization buffer and incubated for 1 h at 49 °C with the Cy5 reporter dye (see supplier recommendations) and increasing quantity of single-stranded DNA target (0 to 300 fmol of PCR product) in a final volume of 17 μL. Post hybridized samples were washed once in 400 μL of 0.5× SSC/0.05% SDS (4 min at room temperature, 400 rpm), three times in storage buffer, and finally rinse in 400 μL of TE buffer before flow cytometry analysis. The fluorescent background noise was evaluated for each concentration and calculated with QDEM bioconjugates. QDEMs fluorescent codes were detected with the detector channel 1 (0 nm and 525 nm emission) simultaneously with the hybridization signal detected in the channel 4 (Cy5 emitting at 670 nm) of the flow cytometer.

Data Analysis

Flow Cytometry Data

Flow cytometry data were analyzed with WinMDI 2.8 (The SRI, CA, USA). The median fluorescent intensity (MFI in arbitrary unit, a.u.), the geometric mean (Gmean in a.u.) and the percentage (%) of events (%Events), were collected on populations gated with the region defined by the control population. The relative variation of QDEM fluorescent code, %MFI, was calculated as a percentage of the MFI of the sample tested versus the corresponding initial fluores-

cence of the QDEM control population. The relative percentage of events, %rEvents, was calculated similarly using the %Events recorded during sample analysis divided by the %Events of the control population. The QDEM stock solution was used as a control to define the gate and its MFI was used to control QDEM specific fluorescent code.

The corrected MFI, RMFI (in a.u.), of the hybridization signal was calculated by subtracting the background signal detected with the negative controls to the positive samples. The background signal was determined for each batch conjugation experiment with QDEM incubated with the probes but without the carbodiimide activators. Three replicates were run per experiment. Flow cytometry Data are presented as the mean of replicates±standard error.

Curves and statistics were calculated with GraphPad Prism5.01 (GraphPad Software, San Diego, CA, USA).

Quantification and Titration Curve

The QuantiBRITE Phycoerythrin bead kit (Becton Dickinson, BD biosciences, Oxford, UK) was used as previously described to evaluate the molecules of equivalent soluble fluorochrome (MEF) [17, 18]. Corrected MEF (RMEF in number of oligonucleotides) were calculated by subtracting the background signal detected with the negative controls to the positive samples. The oligonucleotide density (D_o) corresponded to the number of fluorescent molecules covering the microsphere surface (in oligo/μm^2) [15]. Data are presented as the mean of replicates±standard error of the mean (±SEM). Curves and statistics were calculated with GraphPad Prism5.01 (GraphPad Software, San Diego, CA, USA).

ANOVA and Statistical Tests

A minimum of 11 replicates was required to test the normality distribution and to undertake comparative tests on the different QDEM population data. Non-encoded and 525 nm-encoded beads bioconjugate replicates were statistically analyzed (GraphPad Prism5.01). For each replicates the control sample was run simultaneously. The number of events and the MFI data of bioconjugate and control were collected on populations gated with the region defined with the control population. A D'Agostino and Pearson normality test was run for each flow cytometer parameter of each population. Populations presenting a Gaussian distribution were analyzed with one-way analysis of variance (ANOVA). Paired t-tests were used to compare QDEM population before and after conjugation for each flow cytometer parameters because the conjugation procedure was repeated more than ten times and because control and treated bead were run in parallel for each replicate. The MFI values of bioconjugates were corrected by subtracting the MFI values of the corresponding controls for each flow cytometer parameters. A D'Agostino and Pearson normality test was then run for each paired corrected data. Populations presenting a Gaussian distribution were analyzed by a paired *t*-test. If the data failed the normality test (p-value< 0.05), a Wilcoxon matched pairs non-parametric *t*-test was used instead.

Light scattering (SSC and FSC) MFI data, and the percentage of events were also compared between control and bioconjugate from 0 to 525 nm-encoded bead populations. These comparisons were not assimilated to a paired experiment, since the bioconjugation experiment for both populations were not undertaken at the same time. The MFI and the %Events data were analyzed separately as they presented different units and order of magnitudes. ANOVA's post analysis evaluates statistical differences among the parameters (SSC, FSC) for non-encoded and 525 nm-encoded beads populations. As only two groups were compared, the Tukey-Kramer's multiple comparison test was not adapted, and a unpaired *t*-test was then performed. The corrected percentage of events for 0 and 525 nm-encoded bead population following a Gaussian distribution was analyzed by an unpaired *t*-test. Data are presented as the mean of the replicates±the standard deviation. The full table of results is reported in Additional file 2.

Acknowledgments This work was funded by Cranfield University. We are grateful to Dr. C. Boisson-Vidal, Dr. J. Warrand, and Dr. S. Dunn for useful discussions. We thank Jenny Crawford from Crystaplex™ (Pittsburgh, PA, USA) for technical support.

References

1. Norris DJ, Efros AL, Rosen M, Bawendi M (1996) Size dependence of exciton fine structure in CdSe quantum dots. Phys Rev B 53:16347–16354
2. Chan WCM, Nie SM (1998) Quantum dot bio-conjugates for ultrasensitive non isotopic detection. Science 281:2016–2018
3. Liu T, Liu B, Zhang H, Wang Y (2005) The fluorescence bioassay platforms on quantum dots nanoparticles. J Fluoresc 15:729–733
4. Medintz I, Uyeda H, Goldman E, Mattoussi H (2005) Quantum dot bioconjugates for imaging, labelling and sensing. Nat Mater 4:435–446
5. Han M, Gao X, Su JZ, Nie S (2001) Quantum dot-tagged microbeads for multiplexed optical coding of biomolecules. Nat Biotechnol 19:613–635
6. Gao X, Nie S (2004) Quantum dot-encoded mesoporous beads with high brightness and uniformity: rapid readout using flow cytometry. Anal Chem 76:2406–2410
7. Wang HQ, Huang ZL, Liu TC, Wang JH, Cao YC, Hua XF, Li XQ, Zhao YD (2007) A feasible and quantitative encoding method for microbeads with multicolor quantum dots. J Fluoresc 17:133–138
8. Salas VM, Edwards BS, Sklar LA (2008) Advances in multiple analyte profiling. Adv Clin Chem 45:47–45

9. Spiro A, Lowe M, Brown D (2000) A bead-based method for multiplexed identification and quantitation of DNA sequences using flow cytometry. Appl Environ Microbiol 66:4258–4265
10. Lowe M, Spiro A, Summers AO, Wireman J (2004) Multiplexed identification and quantification of analyte DNAs in environmental samples using microspheres and flow cytometry. Methods in biotechnology: environmental biology: methods and protocols Edited by Spencer JFT, Spencer ALR. Humana Press, 51–74
11. Xu H, Sha MY, Wong EY, Uphoff J, Xu Y, Treadway JA, Truong A, O'Brien E, Asquith S, Stubbins M, Spurr NK, Lai EH, Mahoney W (2003) Multiplexed SNP genotyping using the Qbead™ system: a quantum dot-encoded microsphere-based assay. Nucleic Acid Res 31(1–10):e43
12. Cao YC, Liu TC, Hua XF, Zhu XX, Wang HQ, Huang ZL, Zhao YD, Liu MX, Luo QM (2006) Quantum dot optical encoded polystyrene beads for DNA detection. J Biomed Opt 11:054025-1-7
13. Huo Q (2007) A perspective on bioconjugated nanoparticles and quantum dots. Colloids Surf B Biointerface 59:1–10
14. Maier JS, Panza JL, Bootman M (2007) Nanocrystal clusters in combination with spectral imaging to improve sensitivity in antibody labeling applications of fluorescent nanocrystals. Prog Biomed Opt Imaging 8:64280-1-11
15. Guo X, Peng J, Yang J, Peng F, Yu H, Wang H (2009) Quantum dot-encoded beads for ultrasensitive detection. Recent Pat Nanotechnol 3:192–202
16. Wittebolle L, Verstuyft K, Verstraete W, Boon N (2006) Optimization of amino-carboxy coupling of oligonucleotides to beads used in liquid arrays. J Chem Tech Biotechnol 27:476–480
17. Pannu KK, Joe ET, Iyer SB (2001) Performance evaluation of QuantiBRITE phycoerythrin beads. Cytometry 45:250–258
18. Clapp AR, Medintz IL, Mauro JM, Fisher BR, Bawendi MG, Mattoussi H (2004) Fluorescence resonance energy transfer between quantum dot donors and dye-labeled protein acceptors. JACS 126:301–310
19. Agrawal A, Deo R, Wang GD, Wang MD, Nie S (2008) Nanometer-scale mapping and single-molecule detection with color-coded nanoparticle probes. Proc Natl Acad Sci USA 105:3298–3303
20. http://www.bangslabs.com/products/bangs/guide.php, Polystyrene fluorescent microsphere, last visited May 2011
21. http://www.luminexcorp.com/prod/groups/…/oligo-coupling-scaling-recom.pdf, Scaling up and scaling down oligonucleotides coupling reaction, p. 1–4, last visited May 2011
22. Wang L, Tan W (2006) Multicolor FRET silica nanoparticles by single wavelength excitation. Nano Lett 6:84–88
23. Peterson AW, Heaton RJ, Georgiadis RM (2001) The effect of surface probe density on DNA hybridization. Nucleic Acids Res 29:5163–5168
24. Pack SP, Kamisetty NK, Nonogawa M, Devarayapalli KC, Ohtani K, Yamada K, Yoshida Y, Kodaki T, Makino K (2007) Direct immobilization of DNA oligomers onto the amine-functionalized glass surface for DNA microarray fabrication through the activation-free reaction of oxanine. Nucleic Acid Res 35:e110
25. Son A, Dosev D, Nichkova M, Ma Z, Kennedy IM, Scow KM, Hristova KR (2007) Quantitative DNA hybridization in solution using magnetic/luminescent core-shell nanoparticles. Anal Biochem 370:186–194
26. Raghavachari N, Bao YP, Li G, Xie X, Müller UR (2003) Reduction of autofluorescence on DNA microarrays and slide surfaces by treatment with sodium borohydride. Anal Biochem 312:101–105
27. Men'shikova AY, Evseeva TG, Chekina NA, Ivanchev SS (2001) Synthesis of polymethyl methacrylate microspheres in the presence of dextran and its derivatives. Russ J Appl Chem 74:489–493
28. Sheng W, Kim S, Lee J, Kim SW, Jensen K, Bawendi MG (2006) In-situ encapsulation of quantum dots into polymer microsphere. Langmuir 22:3782–3790
29. Vijayalakshmi S, Madras G (2004) Effect of temperature on the ultrasonic degradation of polyacrylamide and poly (ethylene oxide). Polym Degrad Stab 84:341–344
30. Shim SE, Ghose S, Isayev AI (2002) Formation of bubbles during ultrasonic treatment of cured poly(dimethyl siloxane). Polymer 43:5535–5543
31. Caruso MM, Davis DA, Shen Q, Odom SA, Sottos NR, White SR, Moore JS (2009) Mechanically-induced chemical changes in polymeric materials. Chem Rev 109:5755–5798
32. Chan Y, Zimmer J, Stroh M, Steckel J, Jain R, Bawendi M (2004) Incorporation of luminescent nanocrystals into monodisperse core-shell silica microspheres. Adv Mater 16:2092–2097
33. Yang DL, Kraght P, Pentoney CS, Pentoney SL Jr (2007) Analytical significance of encroachment in multiplexed bead-based flow cytometric assays. Anal Chem 79:3607–3614
34. Resch-Genger U, Hoffmann K, Nietfeld W, Engel A, Neukammer J, Nitschke R, Ebert B, Macdonald R (2005) How to improve quality assurance in fluorometry: fluorescence-inherent sources of error and suited fluorescence standards. J Fluoresc 15:337–362
35. Wu Y, Campos SK, Lopez GP, Ozbun MA, Sklar LA, Buranda T (2007) The development of quantum dot calibration beads and quantitative multicolor bioassays in flow cytometry and microscopy. Anal Biochem 364:180–192
36. Tycko DH, Metz MH, Epstein EA, Grinbaum A (1985) Flow-cytometric light scattering measurement of red blood cell volume and hemoglobin concentration. Appl Opt 24:1355–1365
37. Horejsh D, Martini F, Poccia F, Ippolito G, Di Caro A, Capobianchi M (2005) A molecular beacon, bead-based assay for the detection of nucleic acids by flow cytometry. Nucleic Acids Res 33:e13
38. Chen J, Iannone MA, Li MS, Taylor JD, Rivers P, Nelsen AJ, Slentz-Kesler KA, Roses A, Weiner MP (2000) A microsphere-based assay for multiplexed single nucleotide polymorphism analysis using single base chain extension. Genome Res 10:549–557
39. Dunbar SA, Jacobson JW (2000) Application of the luminex LabMAP in rapid screening for mutations in the cystic fibrosis transmembrane conductance regulator gene: a pilot study. Clin Chem 46:1498–1500
40. Armstrong B, Stewart M, Mazumder A (2000) Suspension arrays for high throughput, multiplexed single nucleotide polymorphism genotyping. Cytometry 40:102–108
41. Werntges H, Steger G, Riesner D, Fritz HJ (1986) Mismatches in DNA double strands: thermodynamic parameters and their correlation to repair efficiencies. Nucleic Acid Res 14:3773–3790
42. Thiollet S, Bessant C, Morgan LS (2011) Application of multiple response optimization design to quantum dot-encoded microsphere bioconjugates hybridization Assay. Anal Biochem 414:23–30
43. Rozen S, Skaletsky H (2000) Primer3 on the WWW for general users and for biologist programmers. Methods Mol Bio 132:365–386